X-Ray Diffraction from a SiGe Island Quasicrystal

J. Stangl, J. Novak, E. Wintersberger, V. Holy, G. Bauer

Institute for Semiconductor and Solid State Physics, University of Linz, A-4040 Linz

Introduction

Nanometer-sized semiconductor islands and quantum dots have opened up the route to novel optoelectronic and electronic applications. The growth of islands by self-assembly in the Stranski-Krastanow growth mode is a well-established method. In general, self-assembled islands are inhomogeneous in size. An improvement of the size homogeneity can be achieved by growing islands in regular two dimensional (2D) arrays [1] – [5]. Such a 2D island lattice can be extended into a three dimensional (3D) island crystal by stacking island layers separated by spacer layers using appropriate growth conditions [6], [7]. Shape and size of the islands as well as their chemical composition undergo substantial changes during capping mainly due to interdiffusion with the spacer material. Direct images of the morphology of buried islands can be obtained by cross-section transmission electron microscopy (TEM) and scanning tunneling microscopy (STM) (see Ref. [8] and references therein). Alternatively, structural properties of buried islands can be studied by x-ray diffraction (XRD), which yields information on a much larger ensemble of the islands and is particularly sensitive to lattice strains.

We used coplanar high-angle XRD to investigate the size and the chemical composition of Ge/Si islands in a 3D island crystal. The evaluation of the experimental data was based on calculations of diffusely scattered intensity for a model island. For the calculations of the elastic strain fields caused by lattice mismatch between Si and Ge, we refined an analytical solution of continuum elasticity equations, which was used in Refs. [9] – [11] for the calculation of strain fields in two dimensions, for SiGe wires and laterally modulated $InAs_nAlAs_m$ short period superlattices.

Experimental

The investigated sample was grown by solid-source molecular beam epitaxy on Si(001), which was prepatterned with a square grid of pits using electron beam lithography and reactive ion etching. The pit grid is oriented along ⟨110⟩ directions and has a period of 400 nm. The size of the patterned area is 0.5 x 0.5 mm^2. After growth of a 150 nm thick Si buffer layer, further deposition of 6 ML of Ge at 700 °C resulted in 2D ordered islands, with one island per pit. After depositing 30 nm of Si as a spacer layer 12 double-layers of Ge islands and Si spacer layers of about 25 nm were deposited at 650 °C. The topmost island layer was left uncapped for atomic force microscopy (AFM) investigations. The islands grew in the same 2D grid in each island layer due to their preferential nucleation in strain energy minima above the underlying islands in the pits.

A nearly perfect 3D island crystal was produced in this way. Details on growth and atomic force microscopy (AFM) images of the topmost island layer are shown in Ref. [7]. The aspect ratio of the uncapped island sidewalls height/width = 0.2 corresponds to {105} sidewall orientation, which is characteristic for pyramidal islands.

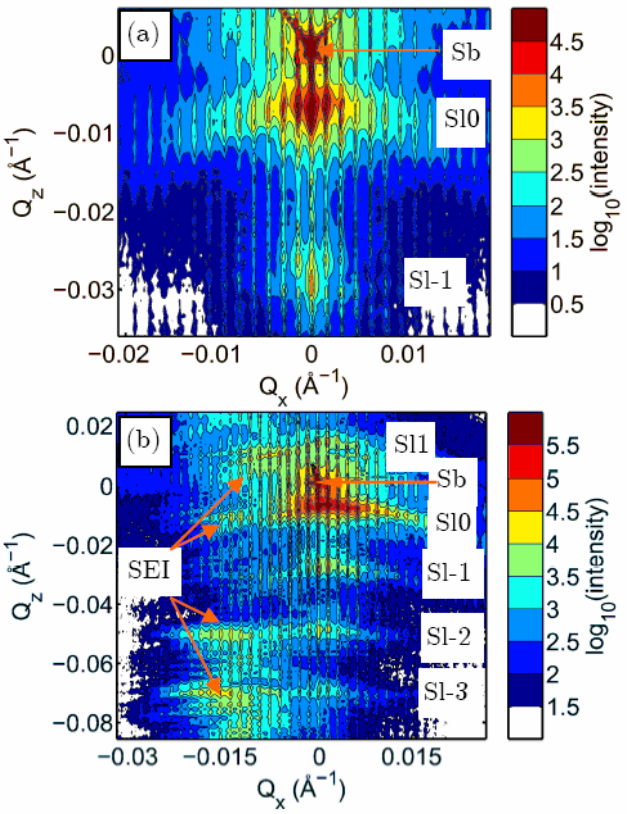

Fig. 1: Measured reciprocal space maps around the (224) (a) and (004) (b) reciprocal lattice points. Vertical satellites, originating from the periodicity of the island layers along the growth direction, are denoted Sl-3 to Sl1. Substrate peaks are denoted by Sb, and SEI denotes stripes of enhanced intensity (see text).

The measurements were carried out at beamline ID10B at the European Synchrotron Radiation Facility (ESRF), Grenoble, at a wavelength of 1.547 Å. High-resolution XRD was measured in coplanar geometry using a Si (111) analyzer in front of a point detector in order to resolve the lateral satellites. Diffusely scattered intensity around the symmetrical (004) and asymmetrical (224) substrate lattice points was measured, the resulting reciprocal space maps (RSMs) are shown in Fig. 1. The Si substrate peaks are denoted by Sb, horizontal stripes of enhanced intensity, denoted Sl-3 to Sl1 in Fig. 1, are vertical satellites due to the periodically repeated motif of island layers / spacer layers. Their distance corresponds to a vertical period of $L_\perp = 30.0 \pm 0.5$ nm.

For the simulations of scattered intensity we used kinematical approximation, as we fitted the intensity distribution beside the crystal truncation rods, where dynamic scattering effects are not important. The expressions used involve the displacement field in the sample, which we calculated by means of an analytic solution of the elasticity equations. We assume that the islands in each island layer form a perfect 2D lattice and that the islands are perfectly stacked above each other. Additionally, the size, shape, and chemical composition of all islands in the 3D island crystal are assumed to be identical. We neglected the uncapped island layer on top of the sample, but rather assume a flat sample surface. In coplanar diffraction geometry, the existence of the uncapped island layer has no significant influence on the scattered intensity.

Due to the lateral periodicity of the island pattern, we performed a Fourier transformation in the expressions of the scattered intensity as well as in the displacement fields and the elastic constants, allowing for an analytic solution of the equilibrium equations of elasticity. Details can be found in Ref. [12].

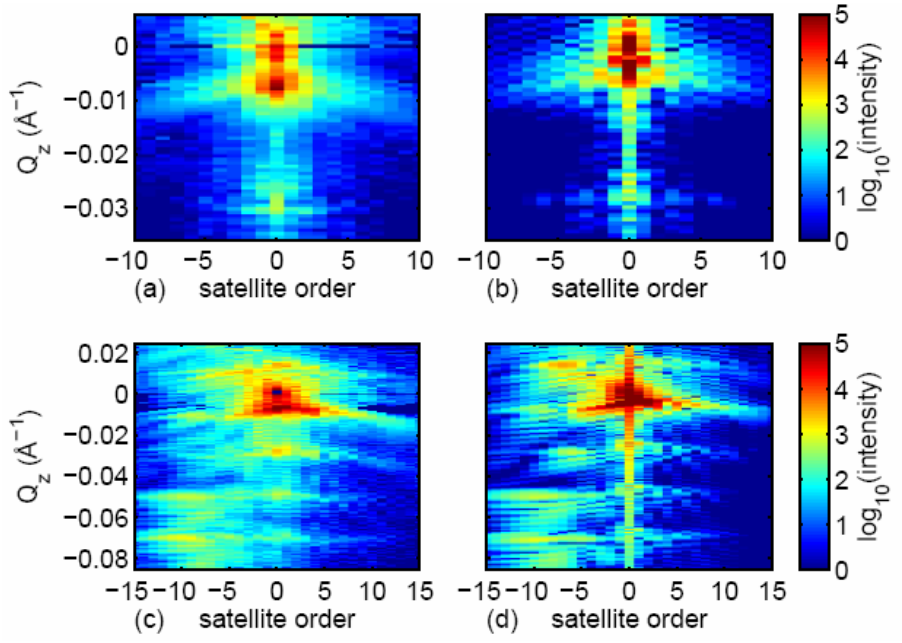

Fig. 2: 2D map of the lateral satellite intensities extracted from RSMs measured around the (004) (a) and (224) (c) reciprocal lattice points. Simulations of diffusely scattered intensity for the (004) (b) and (224) (d) diffractions.

Results

In order to evaluate x-ray data we first fitted the measured intensity profiles along the Q_x axis by series of Lorentzians. Their amplitudes are plotted in Figs. 2 (a), (c) as a function of the satellite order along the [110] direction and Q_z for (004) and (224) diffractions, respectively. The Q_x position of a given lateral satellite order is constant along Q_z, implying vertical replication of the lateral island positions in subsequent layers. The FWHM of the satellites as a function of satellite order is constant and comparable to the instrumental resolution, indicating the excellent long-range order of island positions.

For the simulations of the diffuse intensity and the strain fields all islands were assumed to have the same shape of a truncated cone, characterized by its bottom radius R_{bot}, top radius R_{top}, and height h_i. The Ge content x_i was assumed to be constant within islands. Additionally, a wetting layer (WL) of a constant thickness h_w and a constant Ge content x_w throughout the lateral unit cell was used. A rotational symmetry of the island shape was chosen in accordance with Ref. [13], where the preferential alloying of the island corners due to the surface diffusion of the Si atoms was observed, corresponding to an effective rounding of the islands during capping.

During fitting we made the following observations. (i) The lower the Ge content in the islands, the more intense are the lateral satellites close to the substrate peak. Furthermore, stripes of enhanced intensity within the vertical satellites move closer to the truncation rod. This can be explained by the decrease of the island lattice strain for lower Ge content. (ii) The higher the islands, the further away from the truncation rod the stripes of enhanced intensity are within the vertical satellites. This effect is connected with the larger degree of lattice relaxation in the island layers closer to the top surface. (iii) The vertical shift of the 0^{th} order vertical satellite with respect to the substrate Bragg peak increases with the total amount of Ge in the WL. (iv) Finally, the tilt of the vertical satellites with respect to the Q_x axis increases with the island base radius.

The best simulation (see Figs. 2 (b), (d)) was obtained for island bottom and top radii of R_{bot} = 85 ± 10 nm and R_{top} = 10 ± 10 nm, island height of h_i = 19 ± 4 nm, and a Ge content of x_i = 40 ± 10%. The WL height was h_w = 0.8 nm and its Ge content x_w = 10% (only the product $h_w x_w$ can be determined from the fitting). We obtain an aspect ratio of $\eta = h_i / (R_{bot} - R_{top})$ = 0.25 ± 0.06, close to η = 0.2 of {105} facets typical for Ge pyramids, and different from η = 0.47 of {113} facets typical for Ge domes.

From the simulations also the lateral (ε_{xx}) and vertical (ε_{zz}) strains within the island stack follow (zero strain corresponds to the non-deformed Si lattice). The strain field is almost periodic in the vertical direction only in the region from 4th to 7th island layers; above and below the surface relaxation and influence of the Si substrate destroy the periodicity. The maximum lateral strain of ε_{xx} = 0.9% is observed in compressed SiGe in the top edges of the islands, corresponding to a degree of relaxation of 55% $Si_{0.6}Ge_{0.4}$. The lateral strain minimum of ε_{xx} = –0.5% is observed in compressed Si around the bottom edges of the islands. The vertical strain ε_{zz} increases in the lateral direction from the center of the islands towards their sidewalls. The maximum of ε_{zz} = 3.4% is observed in expanded SiGe in the bottom edge of the islands, and the minimum of ε_{zz} = –2% is observed in compressed Si just above the center of the top island facets.

Conclusion

An analysis of coplanar high-angle x-ray diffraction data was performed and structural information on buried Ge islands was obtained, which form a 3D island crystal. Combining an analytical solution of equilibrium equations of linear elasticity and kinematical scattering theory we successfully simulated the experimental x-ray diffraction data. Comparing the measured reciprocal space maps of the diffracted intensity with simulations, we found that the islands have {105} facets after Si capping, i.e., they have pyramidal shape. The Ge content in the islands is as low as 40 ± 10%. From the fits, also the strain state in and around the buried islands was determined.

References

[1] O.G. Schmidt *et al.*, Appl. Phys. Lett. **77**, 4139 (2000).

[2] G. Jin, J.L. Liu, K.L. Wang, Appl. Phys. Lett. **76**, 3591 (2000).

[3] M. Borgström, V. Zela, W. Seifert, Nanotechnology **14**, 264 (2003).

[4] Bin Yang, Feng Liu, M.G. Lagally, Phys. Rev. Lett. **92**, 25502 (2004).

[5] Zh. Zhong, G. Bauer, Appl. Phys. Lett. **84**, 1922 (2004).

[6] G. Springholz, V. Holý, M. Pinczolits, G. Bauer, Science **282**, 734 (1998).

[7] Zh. Zhong *et al.*, Physica E **21**, 588 (2004).

[8] J. Stangl, V. Holý, G. Bauer, Rev. Mod. Phys. **76**, 725 (2004).

[9] T. Roch *et al.*, Phys. Rev. B **65**, 245324 (2002).

[10] J.H. Li *et al.*, Phys. Rev. B **66**, 115312 (2002).

[11] O. Caha *et al.*, J. Appl. Phys. **96**, 4833 (2004).

[12] J. Novak *et al.*, to be published.

[13] U. Denker, M. Stoffel, O.G. Schmidt, Phys. Rev. Lett. **90**, 196102 (2003).